

JIPipe: Visual batch processing for ImageJ

Marc Figge (✉ Thilo.Figge@leibniz-hki.de)

Leibniz Institute for Natural Product Research and Infection Biology <https://orcid.org/0000-0002-4044-9166>

Ruman Gerst

Leibniz Institute for Natural Product Research and Infection Biology <https://orcid.org/0000-0002-0723-6038>

Zoltan Cseresnyes

Leibniz Institute for Natural Product Research and Infection Biology

Article

Keywords:

Posted Date: May 11th, 2022

DOI: <https://doi.org/10.21203/rs.3.rs-1641739/v1>

License:  This work is licensed under a Creative Commons Attribution 4.0 International License.

[Read Full License](#)

1 *JIPipe*: Visual batch processing for *ImageJ*

2 Ruman Gerst^{1,2,#}, Zoltán Cseresnyés^{1,#}, Marc Thilo Figge^{1,3,*}

3

4 ¹ Applied Systems Biology, Leibniz Institute for Natural Product Research and Infection Biology – Hans
5 Knöll Institute (HKI)

6 ² Faculty of Biological Sciences, Friedrich-Schiller-University Jena, Germany

7 ³ Institute of Microbiology, Faculty of Biological Sciences, Friedrich-Schiller-University Jena, Germany

8 # These authors contributed equally

9 * Correspondence should be addressed to thilo.figge@leibniz-hki.de

10 Abstract

11 The continuous development of new microscopy techniques requires the parallel evolution of image
12 analysis workflows. *ImageJ* provides a high level of accessibility to bioimage processing, which is still
13 impeded by the necessity of developing scripts to achieve reproducibility, and to comply to the FAIR
14 principles. We provide a visual language termed *JIPipe* that allows the construction of an *ImageJ* workflow
15 purely by designing a flowchart. We already included over 1000 functions from *ImageJ* and its plugins. In
16 return, *ImageJ* is extended with custom-designed algorithms, thus forming a symbiotic relationship with
17 *JIPipe*. Our software includes a fully reproduceable and standardized project format, zero-cost scalability
18 of pipelines, as well as automated data saving into an open format. *JIPipe* was already utilized to solve
19 numerous demanding image analysis tasks, showcasing its wide applicability and adaptability. *JIPipe*
20 contributes towards making bioimage analysis more accessible, thereby fostering collaborations between
21 experimentalists and computer scientists.

22 Introduction

23 *ImageJ*¹ is a widely used tool for bioimage analysis² due to its interactive analysis workflow and high
24 extensibility via plugins. Its intuitive graphical user interface (GUI) makes functions easily accessible, even
25 to unexperienced users, while still providing more advanced operations for experts. However, the
26 interactive approach of *ImageJ* has currently two major shortcomings: (1) *ImageJ* does not provide means
27 to ensure analysis in accordance with the FAIR (Findability – Accessibility – Interoperability – Reusability)
28 principles³, where all processing steps and parameters would be tracked automatically rather than relying
29 on researchers' manual notes on all executed steps and their parameters. (2) *ImageJ* does not provide
30 batch processing via the GUI making the analysis of larger projects with hundreds or thousands of datasets
31 time-consuming and error-prone, as every step needs to be executed manually via the GUI. To solve these
32 issues, *ImageJ* includes a macro language that can be used to write fully automated and reproducible
33 pipelines of all functions available inside the GUI. A major disadvantage of such a scripting language is that
34 the development of custom pipelines requires programming experience. Additionally, to comply with the
35 FAIR principles, there is a significant amount of code required to be implemented that reads and manages
36 images and metadata, keeps track of these during the analysis, and exports the results in the desired

37 format. Especially in comparison with the *ImageJ* GUI, writing macros is excessively complex and non-
38 accessible for researchers without programming experience.

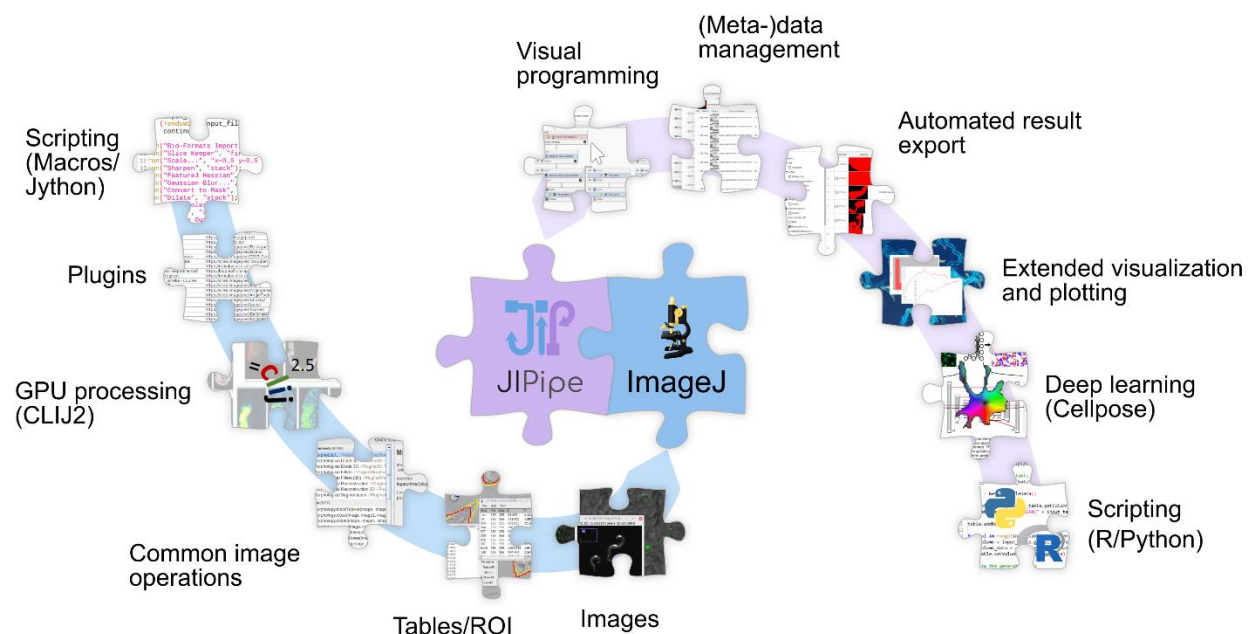
39 In recent years, visual programming languages have been developed in various scientific fields to
40 conveniently solve the aforementioned shortcomings of scripting languages. A well-known example is
41 *KNIME*⁴ that is an open source, visual data analysis environment focusing on general data processing, while
42 community-developed functions handle images. Another example of a visual programming language is
43 available in *Icy*⁵, which provides functionality similar to *KNIME*, whilst focusing exclusively on image
44 analysis and providing methods that allow the application of *ImageJ* commands. Furthermore, *CLIJ*⁶ is a
45 visual language that enables interactive utilization of GPU-based pipelines. Visual languages are as well
46 implemented in commercial languages, for example *Apeer*⁷, applying the concept of customizing machine
47 learning algorithms for image processing. Outside image analysis applications, *Galaxy*⁸ provides a cloud-
48 based visual language for genome sequencing analysis, where web-based image analysis functionality is
49 currently being implemented. In the area of education, *Scratch*⁹ became popular as a graphical software
50 for children to learn programming in an accessible way.

51 All visual programming languages have in common that they provide a GUI for creating a pipeline of nodes
52 that have one or multiple inputs and outputs. These allow for the integration of a node into the pipeline
53 that eventually realizes the automated analysis by the execution of functions in the right order. Such
54 graphical platform is not yet available in *ImageJ*. Therefore, we developed the Java Image Processing
55 Pipeline (*JIPipe*) as a visual programming language that is specifically designed for the *ImageJ* software
56 ecosystem. All functionality that is familiar to *ImageJ* users is as well available in *JIPipe* in form of nodes,
57 including operations on images, regions of interest and tables. *JIPipe* also extends to adapted
58 functionalities that would not be easily achievable in native *ImageJ* methods, including batch visualization,
59 advanced plotting, table processing and automated data export. In other words, *JIPipe* integrates visual
60 programming into the existing *ImageJ* software ecosystem providing a user-friendly way to create
61 reproducible and fully automated pipelines based on *ImageJ*. In addition, *ImageJ* can utilize algorithms
62 and pipelines made for *JIPipe* via the GUI or via macros in analogy to any other plugin. The simplicity of
63 scaling, pipeline building, compartmentalization and automated saving features make *JIPipe* a well-suited
64 environment for *ImageJ* users to create reproducible and scalable workflows. *JIPipe* fills a niche by bridging
65 the gap between researchers¹⁰ with limited programming experience and the advancing development of
66 modern methods of automated image processing. In particular, popular *ImageJ* plugins including
67 *MorphoLibJ*¹¹, *FeatureJ*¹², *CLIJ*⁶, *Multi-Template-Matching*¹³, *OMERO*¹⁴, and *Bio-Formats*¹⁵ can be accessed
68 via *JIPipe*, as well as *Cellpose*¹⁶ to perform deep learning by visual programming. Furthermore, *JIPipe* comes
69 with nodes for *Python*¹⁷, *Jython*¹⁸, *R*¹⁹, and *ImageJ* macro scripts, thus extending the flexibility of workflow
70 development for experienced users with programming skills. *JIPipe* has already been successfully applied
71 to solve numerous image analysis tasks, including recently published works on nematode activity analysis²⁰
72 and the quantification of multispectral optoacoustic tomography (MSOT) images²¹, thus underlining its
73 flexibility and wide applicability.

74 Results

75 **Symbiosis of *ImageJ* and *JIPipe*.** The relationship between *ImageJ* and *JIPipe* is symbiotic in that the two
76 platforms share their functionality (see **Fig. 1**). *JIPipe* incorporates a growing set of already more than 1000
77 functions from *ImageJ* and encapsulates them into features that are suitable for the visual batch
78 processing environment. GUI elements, including manager windows for images, tables, and regions of
79 interest (ROI), are transformed into data objects to lift limitations on the number of instances and to

80 improve the processing speed. Operations on these data, available as menu commands in *ImageJ* are
 81 encapsulated into nodes with standardized interfaces for data transfer and parameters. This comprises
 82 common image processing utilities, including thresholding, extraction of measurements and ROI, as well
 83 as functions provided by popular plugins, including *MorphoLibJ*¹¹, *FeatureJ*¹², *Multi-Template-Matching*¹³,
 84 *OMERO*¹⁴, and *Bio-Formats*¹⁵. We also added support for *CLIJ*⁶ to allow processing of images on graphics
 85 cards with the benefit of significantly increasing the performance. Our visual programming approach
 86 comes with an easy-to-learn interface, and automated and standardized (meta-)data management,
 87 allowing even non-programmers to connect all these familiar functions in batch processing pipelines.
 88 *JIPipe* introduces functionality currently not present in *ImageJ*, including extended visualization methods
 89 designed for batch processing, table processing algorithms, nodes for data and metadata management,
 90 plotting with the widely used *JFreeChart*²² library, and support for deep learning via *Cellpose*. To extend
 91 the flexibility of workflow development, our software also allows users to embed *Python*, *Jython*, *R*, and
 92 *ImageJ* macro scripts. Any functionality designed for *JIPipe* is not exclusive to our software, as any
 93 compatible node is automatically made available to be utilized as an *ImageJ* command. Consequently,
 94 *ImageJ* benefits from *JIPipe*-exclusive operations that include improved visualization functions, table
 95 processing algorithms, plotting, access to *Python* and *R*, as well as *Cellpose*-based segmentation. This
 96 symbiotic relationship additionally simplifies the development of *ImageJ* plugins, as developers can target
 97 the *JIPipe* API to develop a library usable in both *ImageJ* and *JIPipe*.

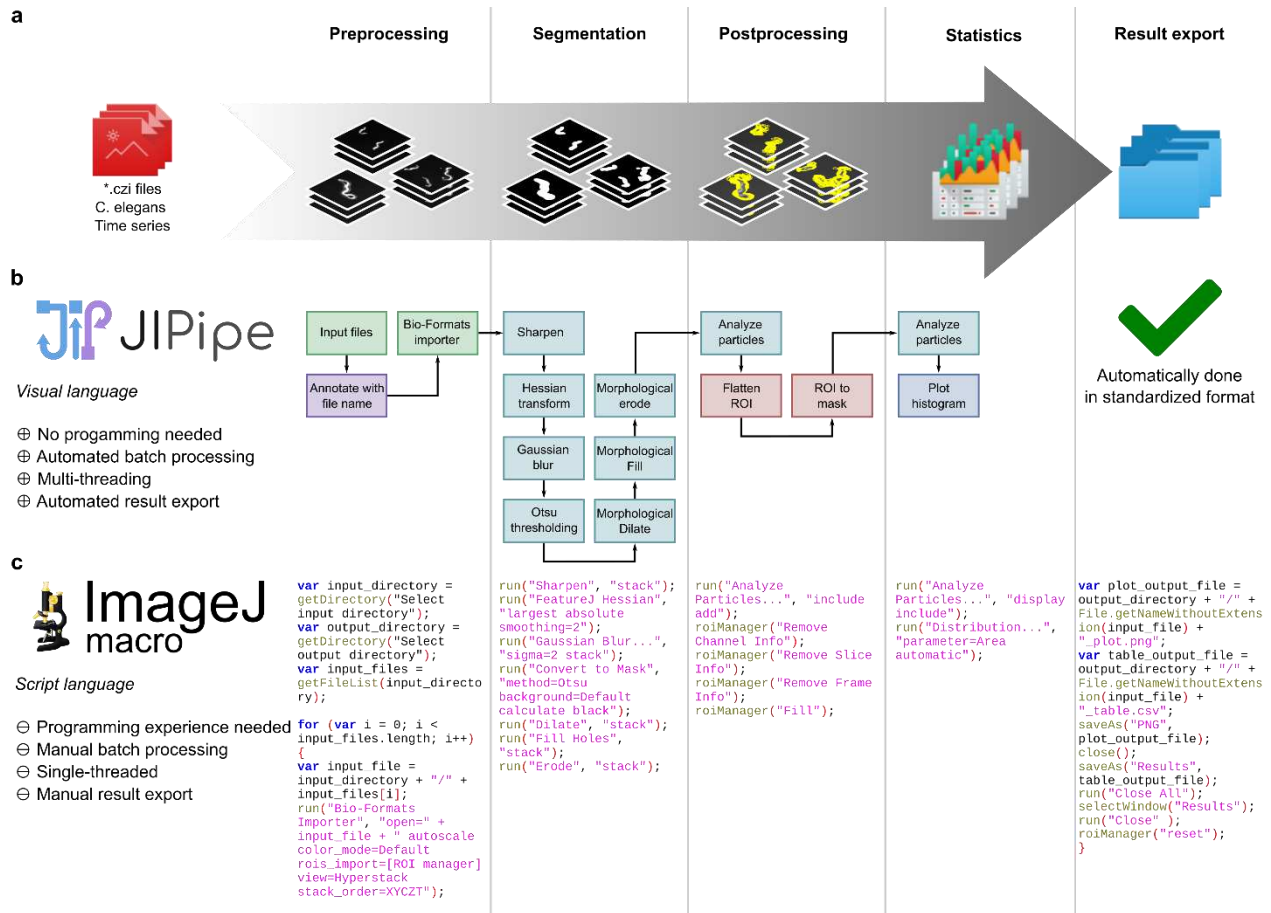


98
 99 **Figure 1** | *JIPipe* and *ImageJ* have a symbiotic relationship where both tools gain access features from each other. *JIPipe*
 100 encapsulates *ImageJ* features, including the manual management of images, tables, and regions of interest into a visual
 101 programming language with automated data management and export. Operations on these data types are available as nodes and
 102 include basic image processing algorithms, and methods from popular plugins, e.g., *CLIJ* for utilizing GPU. *ImageJ* can utilize *JIPipe*
 103 functionalities and has access to extended algorithms for visualization and plotting, and integration of *Cellpose*. *JIPipe* can execute
 104 *ImageJ* macros and *Jython* scripts, while *JIPipe* provides support for *R* and *Python* scripts.

105 *JIPipe* is an easy-to-use alternative to programming *ImageJ* macros, allowing to develop analysis pipelines
 106 within a GUI that are the visual counterpart of macros (see **Fig. 2**). *JIPipe* features include automated batch
 107 processing, parallelization, and result export. The current set of over 1000 available operations can be
 108 extended via plugins that are either provided as Java library or can be created by simply exporting a

109 pipeline as a new node type (see **Supplementary information 1.1** for an overview). As our software already
 110 comes with nodes for scripting languages, a background in Java programming is not needed to integrate
 111 plugins and advanced operations not yet encapsulated into nodes. *JIPipe* stores user-created plugins and
 112 pipelines in an open and standardized format (see **Supplementary information 1.2** and
 113 <https://www.JIPipe.org/> for specifications), making it easy to share workflows with the community on a
 114 level comparable to *ImageJ* macros.

115
 116



117

118 **Figure 2 | Comparison of a batch analysis workflow designed with *JIPipe* versus an equivalent *ImageJ* macro. (a)** The analyzed
 119 image data are time series of 2D+time images showing the moving nematode *C. elegans*²⁰. This particular workflow extracts the
 120 total area covered by *C. elegans* over time from the image files. **(b)** *JIPipe* flowchart that contains the same steps and edges as a
 121 *JIPipe* project that applies the analysis (see **Supplementary information 5d**). *JIPipe* automatically saves all results in a standardized
 122 format (green check mark).

123 **Hallmarks of *JIPipe* by representative applications.** *JIPipe* applications share a set of common features,
 124 including file operations, data management and annotations, table processing, visualization, plotting, and
 125 saving. The graphical workflow editor allows the arrangement of parameterized nodes into
 126 compartmentalized pipelines (**Supplementary Figures 3.1-3.7**) that implement zero-cost scalability due to
 127 a table-based "one node -- multiple data" (meta-)data management (**Supplementary Figure 3.7**).
 128 Compartments are logical units that can be fully flexibly arranged within a dedicated interface, although
 129 they are often arranged according to the preprocessing–analysis–postprocessing–visualization workflow

130 (Supplementary Figures 2.1–2.5, Supplementary information 3, Supplementary Figures 3.1-3.6).
131 Typically, the preprocessing compartment is responsible for file loading and image quality enhancement,
132 as well as channel separation of multichannel images. The analysis compartment carries out the
133 segmentation, masking, and ROI correlation tasks in a channel-specific or conditional way. The outcome is
134 passed on to the postprocessing and visualization compartments (Supplementary information 2.1-2.5).

135 We exemplified the hallmarks of developing image analysis workflows on a set of representative and
136 diverse biological systems that are summarized in Figure 3. For instance, the analysis of microfluidic
137 droplets succeeded at characterizing the extent of bacterial growth under various environmental
138 conditions set up inside these picoliter bioreactors (Fig. 3 row 1)²³. Determining the organ-wide
139 distribution of nanocarrier-delivered drugs into the liver of the mouse was the goal in the next example
140 (Fig. 3 row 2)²⁴. The motility ratio of nematodes characterized the survival of earth worms that consumed
141 soil-beneficial fungi either with or without endosymbiotic bacteria (Fig. 3 row 3)²⁰. 3D analysis of big
142 volume data was applied to characterize the morphology and spatial distribution of glomeruli in mouse
143 kidneys (see Fig. 3 row 4)²⁵. Confrontation assays between immune cells and pathogens were quantified
144 by calculating phagocytic measures (Fig. 3 row 5)²⁶. The various types of image data generated for all these
145 representative biological systems were analyzed in *JIPipe* by exploiting the following features:

146 *Deep learning–based image segmentation.* The identification of cell-like objects in both transmitted light
147 (TL) and fluorescence-based images was simplified with the advent of the *Cellpose* framework¹⁶. *JIPipe*
148 adopted this technique by encapsulating both the training and application of *Cellpose* into nodes, as well
149 as Python environment management tools that allow its fully automated setup. The node extracts the
150 gradient flows (Fig. 3 A-1 top left, Fig. 3 A5), the probability map (Fig. 3 A-1 bottom right) and the
151 segmented ROIs (Fig. 3 D-1, D-5). These outcomes of the analysis indicate that the *JIPipe* integration
152 worked well for TL images of microfluidic droplets (see Fig. 3 row 1; Supplementary information 2.1) as
153 well as for images of confrontation assays (see Fig. 3 row 5; Supplementary information 2.3).

154 *Multidimensional image analysis and object tracking.* Nodes dedicated to handling multidimensional
155 datasets were utilized when analyzing nanocarrier-based drug delivery kinetics in intravital microscopy of
156 the liver (see Fig. 3 B-2; Supplementary information 2.2), time series TL data of live nematodes (see Fig. 3
157 B-3; Supplementary information 2.4), and the analysis of big volume 3D image stacks as shown in the
158 example of analyzing light-sheet microscopy data of the kidney (Figure 3 B-4; Supplementary information
159 2.5). To this end, these include operations for automated splitting and merging of multi-dimensional data,
160 as well as functionality provided by existing *ImageJ* plugins.

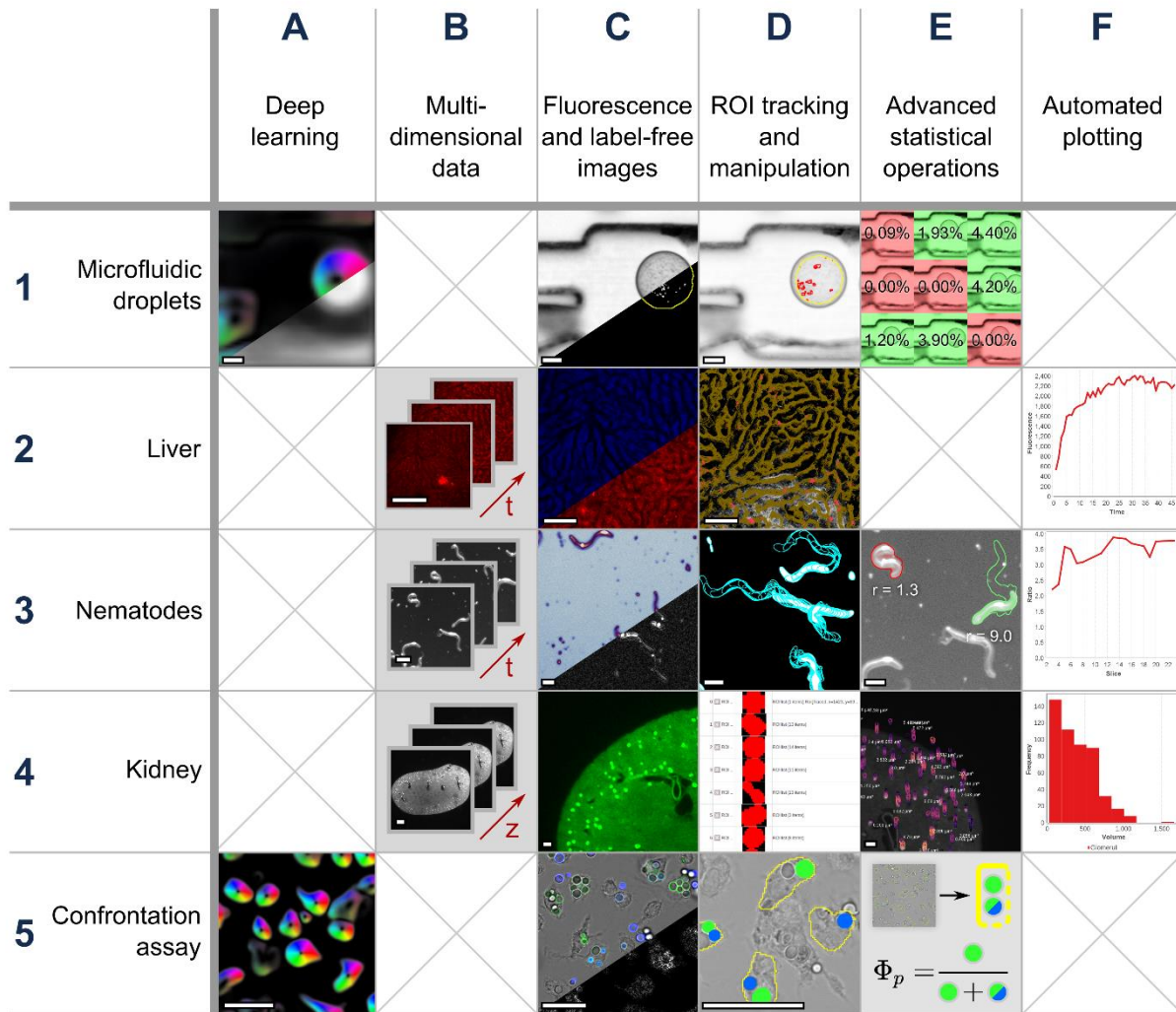
161 *Label-free and fluorescence-based image analysis.* *JIPipe* supplies a complete set of tools to analyze TL and
162 fluorescence-based microscopy data. Hessian filtering was utilized to identify the outline of microfluidic
163 droplets (Figure 3 C-1, Supplementary information 2.1), nematodes (Figure 3 C-3, Supplementary
164 information 2.4), and unlabeled macrophages in confrontation assays (Figure 3 C-5, Supplementary
165 information 2.3). *JIPipe* provides all basic analysis nodes, including blurring, global and local thresholding,
166 morphological operations, watershed algorithms, image normalization and illumination correction, as well
167 as ROI-handling. These tools were applied during the analysis of bacterial growth in microfluidic droplets
168 (Figure 3 C-1, Supplementary information 2.1), liver-targeted drug delivery by nanoparticles (Figure 3 C-
169 2, Supplementary information 2.2), glomeruli identification and quantification in kidney light-sheet
170 microscopy images (Figure 3 C-4, Supplementary information 2.5), as well as labelled fungal spore
171 segmentation (Figure 3 C-5, Supplementary information 2.3).

172 *ROI tracking and manipulation.* More complex segmentation tasks are also supported by nodes designed
173 for ROI operations including functions provided by *ImageJ* and additional nodes that make use of *JIPipe*'s
174 exclusive functionality. These features are utilized in examining i) the extent of bacterial growth inside
175 microfluidic droplets (see **Fig. 3 D-1, Supplementary information 2.1**), where the growth area search had
176 to be limited to within the droplet region; ii) the number of dye-loaded liver sinusoidal endothelial cells
177 (LSECs; see **Fig. 3 D-2, Supplementary information 2.2**), where masking operations limited the search to
178 be carried out only in the immediate vicinity of the sinusoids; iii) the total area touched by migrating
179 nematodes (see **Fig. 3 D-3, Supplementary information 2.4**) where the individual nematode ROIs were
180 merged into the footprint that characterized the motility of the worms; iv) the kidney light-sheet images
181 where ROI-merging via a 3D-connected-components algorithm allowed the volumetric characterization of
182 kidney status under physiological and pathological conditions (see **Fig. 3 D-4, Supplementary information**
183 **2.5**); v) the distribution of phagocytosed fungal conidia where the ROIs describing the fungal spores were
184 examined for their overlap with those of the macrophages to identify phagocytosed and adherent fungi
185 (see **Fig. 3 D-5, Supplementary information 2.3**).

186 *Advanced statistical operations.* *JIPipe* extends the functionality of *ImageJ* with operations for filtering,
187 merging, and manipulating tabular data via user-friendly nodes as well as *Python* and *R* scripts. These were
188 used to calculate percentage growth area of bacteria in microfluidic droplets to identify growth and no-
189 growth classes of the samples (see **Fig. 3 E-1, Supplementary information 2.1**). The total footprint covered
190 by a worm divided by the area of the worm at each time point characterized the viability of the nematodes,
191 here showing an example of a low-motility and a high-motility nematode (ratio = 1.3 and 9.0, respectively)
192 (see **Fig. 3 E-3, Supplementary information 2.4**). The volumes of individual glomeruli were calculated from
193 the axially merged ROIs in the kidney and plotted in the vicinity of the object (see **Fig. 3 E-4, Supplementary**
194 **information 2.5**). Finally, the calculation of various phagocytic measures from the number of overlapping
195 ROIs was made easy by per-row table manipulations, as demonstrated for the phagocytosis ratio (see **Fig. 3**
196 **D-5, Supplementary information 2.3**).

197 *Automated plotting.* Analysis results of a fully or partially executed workflow can be plotted automatically
198 as supported by a set of dedicated nodes. These provide many graph formats that can be further
199 manipulated in a GUI or via the node parameters. The delivery of nanoparticle-linked drugs to the
200 hepatocytes was described by the kinetic curve of the cargo-linked average fluorescence value (see **Fig. 3**
201 **F-2, Supplementary information 2.2**). The instantaneous motility of individual worms was calculated and
202 plotted for the duration of the observation (see **Fig. 3 F-3, Supplementary information 2.4**), whereas a
203 histogram plot of the glomeruli volume distribution characterized the health status of the kidney sample
204 based on its glomeruli number and size (see **Fig. 3 F-4, Supplementary information 2.5**).

205 These examples demonstrate that *JIPipe* greatly complements *ImageJ* by simplifying the management of
206 a multitude of complex image analysis and management tasks.



207

208 **Figure 3** | Examples of biological applications and hallmarks of *JIPipe*. The rows are arranged according to the biological samples,
209 whereas the columns correspond to sets of main features of the *JIPipe* platform. The highlighted techniques include deep learning
210 (**column A**), the handling of multidimensional images (**column B**), the analysis of label-free and fluorescence microscopy data
211 (**column C**), the flexible tools of region of interest (ROI) tracking and manipulations (**column D**), mathematical and statistical
212 operations (**column E**), and data plotting via automatable nodes (**column F**). The rows show examples from the analysis of
213 microfluidic droplets (**row 1**), intravital microscopy of the liver (**row 2**), time-tracking of live nematodes (**row 3**), the segmentation
214 and quantification of kidney glomeruli (**row 4**), and the analysis of confrontation assays between macrophages and fungal spores
215 (**row 5**). (**A-1**) The gradient flow (top left) and probability map (bottom right) of microfluidic droplets, provided by the *Cellpose*
216 algorithm. (**A-5**) The gradient flow of unlabeled macrophages provided by the *Cellpose* node output. (**B-2**) Representative images
217 from a time series of fluorescence images recorded from live liver. (**B3**) Earth worms in transmitted light microscopy images during
218 a time series microscopy experiment. (**B-4**) Selected z slices of a 3D light-sheet microscopy image of mouse kidney. (**C-1**)
219 Microfluidic droplets in a TL image (top left), as well as after segmentation of the droplet inner area (bottom right, yellow line)
220 and of the bacteria (bottom right, white speckles). (**C-2**) Images of autofluorescence (top left, blue) and cargo-linked fluorescence
221 labeling (bottom right, red) of a liver sample during intravital microscopy. (**C-3**) Nematodes in a live time-series TL microscopy
222 experiment before processing (top left, “BuPu” look-up table²⁷) and after Hessian filtering (bottom right). (**C-4**) One z slice of a 3D
223 fluorescence microscopy image of mouse kidney (light green), overlaid with a maximum intensity z projection of the segmented
224 glomeruli ROIs (bright green speckles). (**C-5**) TL images of a confrontation assay (top left) with the macrophages shown in grey,
225 the phagocytosed spores shown in green, and the external conidia presented in blue. The macrophages were identified without
226 fluorescence labeling by applying a Hessian filter (bottom right). (**D-1**) A microfluidic droplet imaged via TL microscopy, with the
227 segmented inner line of the droplet shown in yellow, and the bacterial growth indicated by red. (**D-2**) Mouse liver as revealed by

228 intravital microscopy, showing the sinusoids as a time series maximum projection (dark yellow) superimposed with the time-series
229 projection of LSECs (red speckles). (D-3) The time superposition of nematode outlines during a TL microscopy experiment (blue:
230 nematode outlines at consecutive time points, white: binary image of segmented worms). (D-4) A selection of detected 3D ROIs
231 representing individual glomeruli from a light-sheet microscopy experiment displayed in the JIPipe cache GUI. (D-5) The outline
232 of segmented macrophages (yellow) superimposed with phagocytosed conidia (green) and adherent spores (blue). (E-1) Bacterial
233 growth levels about 0.5% area/area were classified as positive growth (green hue), whereas lower values than 0.5% were
234 considered as negative growth (red hue). The superimposed numbers indicate the per-droplet growth percentage values. (E-3)
235 Nematodes imaged with TL microscopy, recorded as part of a time series. The red and green outlines are the footprints of two
236 individual worms, one each with low and high motility values (red, motility ratio at 1.3; green, motility ratio at 9.0). (E-4) The
237 volume values of individual glomeruli are calculated from light-sheet microscopy images of the mouse kidney. The original image
238 appears as a greyscale background, the ROIs of the segmented glomeruli are shown in perspective view as generated by a special
239 *JIPipe* node, where the individual 2D ROIs are colored according to their z position, and the volume values are printed in white.
240 (E-5) Representation of the principle behind calculating the phagocytosis ratio from confrontation assay images. The segmented
241 macrophages (yellow outline) were matched against the green and blue-labelled conidia in order to find the phagocytosed (green)
242 and adherent (blue) spores. Using the *JIPipe* table calculator node, the ratio of the phagocytosed conidia over the total number
243 of spores (phagocytosed plus adherent) was determined (Φ_p). (F-2) Using *JIPipe's* automated plotting nodes, the mean
244 fluorescence value of the cargo-linked dye measured in the hepatocytes was presented for a time series experiment (red curve).
245 (F-3) The motility ratio of an individual worm was plotted over the course of a time series experiment (red curve). The ratio was
246 defined as the total footprint of the worm covered during the video divided by the area of the worm at each time point. (F-4)
247 Histogram representation of the glomeruli volume for a light-sheet microscopy image set measured in a mouse kidney.
248 Scalebars represent 200 μm in column B, 100 μm elsewhere.

249 ***JIPipe* user interface and data model.** Here we will provide a brief overview of some of the technical details
250 of *JIPipe*, whereas the full organization of our software can be retrieved from the Supplementary Material
251 (3: “*JIPipe* user interface and data model”), as well as from the *JIPipe* website (<http://www.JIPipe.org/>).
252 Whilst *JIPipe* builds upon *ImageJ* functionality, it also contributes its own solution for handling (meta-)data
253 and encapsulating it into a GUI. *JIPipe's* backbone is a directed acyclic graph (DAG) that organizes all
254 functional units, the so-called nodes. A pipeline is formed by connecting nodes through their input and
255 output slots, thus modelling the flow of data. We simplified this concept by the introduction of
256 compartmentalization, which clearly separates projects with a large number of nodes into functional units.
257 *JIPipe* provides over 1000 nodes that cover every core aspect of image analysis and data management,
258 and can be easily searched by name, functionality, and compatibility to the preceding node. To simplify
259 the creation of workflows, many nodes were manually provided with integrated documentation and
260 customization options, for example to test multiple parameter sets, or to apply calculations via user-
261 defined mathematical expressions. These features are made possible by the table-based data
262 management that enforces constraints, for example on data types, presence of a primary data column, or
263 type of annotations. The consequence of a simplified table is zero-cost scaling, meaning that *JIPipe*
264 workflows can be adapted to batch processing without any changes to the pipeline structure. At the same
265 time, a table allows for great flexibility and can be utilized to track biological conditions, dataset identifiers,
266 or image properties, thus providing an easy way to find and reproduce data and analysis details according
267 to the FAIR principles³. According to the symbiotic relationship detailed earlier, all nodes and *JIPipe*
268 algorithms can also be directly accessed from *ImageJ*. Pipelines can be executed in their entirety or up to
269 a user-specified node, with the option of saving the results into a memory cache or on the hard-drive in a
270 standardized format, including all parameters and the complete project file. This allows *JIPipe* to open
271 existing results, making further processing and plotting at a later timepoint possible.

272 In conclusion, *JIPipe* is a user-friendly and powerful tool that introduces visual programming into *ImageJ*.
273 Users who are already familiar with the *ImageJ* software find equivalent functionalities and can continue
274 to use their existing scripts, in both *JIPipe* and *ImageJ*. Batch analyses can be designed efficiently by laying
275 out the steps for a single analysis and then increasing the set of input files – all required functionality to

276 track datasets during the analysis are handled by the powerful table-based data architecture. We showed
277 by the examples presented in **Fig. 3** that *JIPipe*, like *ImageJ*, can be applied to virtually all kind of biological
278 data. *JIPipe* is fully open-source and licensed under BSD-2. Detailed user guides, tutorials, videos,
279 examples, and instructions for developers are available on <https://www.JIPipe.org/>. We are working with
280 the image analysis community (<https://forum.image.sc/>) to further improve *JIPipe* and establish the
281 software as meaningful contribution to collaborative environments.

282 Discussion

283 With the advent of visual programming in many application fields, the need for a visual language for *ImageJ*
284 programming has become apparent. This motivated us to develop *JIPipe* and by that fill a niche that bridges
285 the gap between researchers with limited programming experience and the advancing development of
286 modern methods of automated image processing, including deep learning approaches, parallel- and cloud
287 computing. *ImageJ*¹ gained immense popularity² amongst biologists and bioimage informaticians due to
288 its very wide applicability, ease of use and of expansion, and open-source nature. When it comes to
289 analyzing large amounts of images, especially in a complex structure due, e.g., to a wide set of biological
290 conditions, pipelines in *ImageJ* become complex, making it difficult to record the individual steps and their
291 parameters according to the FAIR principles³. The necessity to have certain programming knowledge to
292 turn single-image analysis workflows into complex batch analysis via macro or plugin programming
293 discourages many less experienced users from developing automated pipelines in *ImageJ*. Here we
294 identified the niche, where our contribution to visual programming can be meaningful for the image
295 analysis community. With *JIPipe*, we established such a visual programming environment, where current
296 *ImageJ* users can utilize their existing knowledge of *ImageJ* to convert existing pipelines into fully
297 automated batch-processing workflows that generate exactly the same results as the *ImageJ* equivalents.

298 At this stage, *JIPipe* focuses on implementing the first version of the *ImageJ* API (*ImageJ1*)²⁸, because the
299 majority of functions in the *ImageJ* GUI still rely on *ImageJ1*, where only one non-standardized string is
300 available for transferring algorithm parameters. In addition, there is a concept of a single “active image”,
301 a single table of results and ROI manager — restrictions that are not compatible with visual programming.
302 In addition, custom GUI components are not suitable for GUI-free and parallel-execution environments.
303 For this reason, we manually curated these functionalities into *JIPipe* nodes, instead of applying an
304 automated algorithm for the conversion. Functions were added, merged, or split into multiple nodes,
305 whereas the concepts of image windows, result tables and ROI manager were adapted into data types
306 compatible with visual programming. As a result, *JIPipe* functions cover the same or very similar tasks as
307 the corresponding commands in *ImageJ*. Due to this conversion process, it was not always sensible to keep
308 the same function names as in *ImageJ*, adding a small learning curve to *JIPipe*. To ease this transition phase,
309 we provide integrated search options, numerous application examples with complete code and data, as
310 well as a thorough online training material (see **Supplementary Information 4**,
311 <https://www.JIPipe.org/tutorials/>).

312 *ImageJ* incorporates a second, more modern API, *ImageJ2*, which is richer in features. For example, there
313 are standardized interfaces for data and parameters, flexible service-based architecture, as well as
314 individually addressable parameters. We adapted our approach of curating the integration via *ImageJ2* by
315 incorporating the Multi-Template-Matching plugin¹³. An automated integration of all compatible
316 operations was achieved by interfacing with the *ImageJ* Ops API² and applying on-demand conversion
317 between *JIPipe* and *Image2* data.

318 In terms of documentations, *JIPipe* adopts the principle of immediate access to all functionality
319 descriptions, greatly simplifying visual programming. The automated documentation tool was built from
320 manually recovered online *ImageJ* documentation and source code, and it is available directly from the
321 nodes.

322 Two of the most established and best-known visual applications in image analysis are *Icy* and *KNIME*. These
323 tools integrate certain aspects of *ImageJ* into their own framework, while *ImageJ* cannot use functions
324 designed for these tools, thus lacking the symbiotic relationship with *ImageJ*. This means that *ImageJ* itself
325 is not the main focus of operation for these visual applications. Consequently, a niche was open for an
326 application that would provide (i) a GUI for *ImageJ* operations with easy batch processing, automated
327 saving, maintained full compatibility with *ImageJ*, (ii) a learning curve that makes this new language
328 accessible for non-programmers, and (iii) a standardized project format that saves all information about
329 the progress and implementation of the project according to the FAIR principles. This niche is filled by
330 *JIPipe*.

331

332 Methods

333 **Software development.** *JIPipe* was developed in Java version 8 and utilizes software libraries provided by
334 *ImageJ* and other developers. A full list of all dependency libraries is given in **Supplementary Table 5.1**,
335 whereas the system requirements are listed in **Supplementary Information 5.2**.

336 **Software availability.** The version of *JIPipe*, and its source code used in this paper is available as
337 supplement. The newest version of *JIPipe* and the current version of the source code are available on our
338 website <https://www.JIPipe.org/> and on <https://www.github.com/applied-systems-biology/JIPipe/>
339 (<https://doi.org/10.5281/zenodo.6532719>). *JIPipe* is also available from within the *ImageJ* update service.
340 Instructions are available on our website.

341 **Data availability.** The data that supports our findings are available as supplements. This is also the case
342 for the project files and example data used to demonstrate the usage of *JIPipe*. The example pipelines are
343 available at <https://doi.org/10.6084/m9.figshare.19733320.v1>.

344

345 Acknowledgements

346 This work was financially supported by the International Leibniz Research School for Microbial and
347 Biomolecular Interactions Jena – ILRS Jena. Furthermore, the German Research Foundation (DFG) funded
348 this project through the Collaborative Research Center PolyTarget 1278 – project number 316213987,
349 subproject Z01. This work was also supported by the Collaborative Research Center Funginet 124 – project
350 number 210879364, subproject B4 – and by the Cluster of Excellence “Balance of the Microverse” under
351 Germany’s Excellence Strategy – EXC 2051 – Project-ID 390713860, as well as by the Leibniz
352 ScienceCampus *InfectoOptics* Jena, which is financed by the funding line Strategic Networking of the
353 Leibniz Association. Furthermore, we received support from the Federal Ministry of Education and
354 Research, Germany (grant number 13GW0456B) in the context of the *InfectoGnostics* Research Campus
355 Jena. We are particularly thankful to Dr. Martin Roth (microfluidic droplets data), Prof. Christian Hertweck
356 (nematode imaging), Drs. Kerstin Voigt and Mohamed Hassan (confrontation assay images), Dr. Adrian

357 Press (intravital liver microscopy data), and Prof. Matthias Gunzer (kidney light-sheet images) for kindly
358 providing image data.

359 Author contributions

360 R.G. developed the software. Z.C. designed the bioimage analysis pipelines and tested the software. M.T.F.
361 and Z.C. conceived the idea. M.T.F. directed and supervised the project. All authors wrote the initial draft,
362 read and contributed to the paper and approved the content.

363 References

- 364 1. Rueden, C. T. *et al.* ImageJ2: ImageJ for the next generation of scientific image data. *BMC*
365 *Bioinformatics* **18**, 529 (2017).
- 366 2. Schroeder, A. B. *et al.* The ImageJ ecosystem: Open-source software for image visualization,
367 processing, and analysis. *Protein Sci.* **30**, 234–249 (2021).
- 368 3. Wilkinson, M. D. *et al.* The FAIR Guiding Principles for scientific data management and stewardship.
369 *Sci. Data* **2016 31 3**, 1–9 (2016).
- 370 4. Berthold, M. R. *et al.* KNIME: The Konstanz Information Miner. in *Studies in Classification, Data*
371 *Analysis, and Knowledge Organization (GfKL 2007)* (Springer, 2007).
- 372 5. de Chaumont, F. *et al.* Icy: an open bioimage informatics platform for extended reproducible
373 research. *Nat. Methods* **9**, 690–696 (2012).
- 374 6. Haase, R. *et al.* CLIJ: GPU-accelerated image processing for everyone. *Nat. Methods* **17**, 5–6 (2020).
- 375 7. APEER. <https://www.apeer.com/>.
- 376 8. Afgan, E. *et al.* The Galaxy platform for accessible, reproducible and collaborative biomedical
377 analyses: 2018 update. *Nucleic Acids Res.* **46**, W537–W544 (2018).
- 378 9. Maloney, J., Resnick, M., Rusk, N., Silverman, B. & Eastmond, E. The Scratch Programming Language
379 and Environment. *ACM Trans. Comput. Educ.* **10**, 16:1-16:15 (2010).
- 380 10. Martins, G. G. *et al.* Highlights from the 2016-2020 NEUBIAS training schools for Bioimage
381 Analysts: a success story and key asset for analysts and life scientists. *F1000Research* **10**, (2021).
- 382 11. Legland, D., Arganda-Carreras, I. & Andrey, P. MorphoLibJ: Integrated library and plugins for
383 mathematical morphology with ImageJ. *Bioinformatics* **32**, 3532–3534 (2016).

- 384 12. Meijering, E. FeatureJ. <https://imagescience.org/meijering/software/featurej/>.
- 385 13. Thomas, L. S. V. & Gehrig, J. Multi-template matching: a versatile tool for object-localization in
386 microscopy images. *BMC Bioinformatics* **21**, 44 (2020).
- 387 14. Allan, C. *et al.* OMERO: flexible, model-driven data management for experimental biology. *Nat.*
388 *Methods* **9**, 245–253 (2012).
- 389 15. Linkert, M. *et al.* Metadata matters: access to image data in the real world. *J. Cell Biol.* **189**, 777–
390 782 (2010).
- 391 16. Stringer, C., Wang, T., Michaelos, M. & Pachitariu, M. Cellpose: a generalist algorithm for cellular
392 segmentation. *Nat. Methods* **18**, 100–106 (2021).
- 393 17. Python. <https://www.python.org/>.
- 394 18. Jython. <https://www.jython.org/>.
- 395 19. R Core Team & others. R: A language and environment for statistical computing. (2013).
- 396 20. Büttner, H. *et al.* Bacterial endosymbionts protect beneficial soil fungus from nematode attack.
397 *Proc. Natl. Acad. Sci. U. S. A.* **118**, 2110669118 (2021).
- 398 21. Hoffmann, B. *et al.* Spatial quantification of clinical biomarker pharmacokinetics through deep
399 learning-based segmentation and signal-oriented analysis of MSOT data. *Photoacoustics* **26**, 100361
400 (2022).
- 401 22. JFreeChart. <https://jfree.org/jfreechart/>.
- 402 23. Svensson, C. M. *et al.* Coding of Experimental Conditions in Microfluidic Droplet Assays Using
403 Colored Beads and Machine Learning Supported Image Analysis. *Small* **15**, 1802384 (2019).
- 404 24. Muljajew, I. *et al.* Stealth Effect of Short Polyoxazolines in Graft Copolymers: Minor Changes of
405 Backbone End Group Determine Liver Cell-Type Specificity. *ACS Nano* **15**, 12298–12313 (2021).
- 406 25. Klingberg, A. *et al.* Fully Automated Evaluation of Total Glomerular Number and Capillary Tuft
407 Size in Nephritic Kidneys Using Lightsheet Microscopy. *J. Am. Soc. Nephrol. JASN* **28**, 452–459 (2017).

- 408 26. Cseresnyes, Z., Kraibooj, K. & Figge, M. T. Hessian-based quantitative image analysis of host-
409 pathogen confrontation assays. *Cytometry A* **93**, 346–356 (2018).
- 410 27. Hunter, J. D. Matplotlib: A 2D graphics environment. *Comput. Sci. Eng.* **9**, 90–95 (2007).
- 411 28. Schneider, C. A., Rasband, W. S. & Eliceiri, K. W. NIH Image to ImageJ: 25 years of image analysis.
412 *Nat. Methods* **9**, 671–675 (2012).
- 413

Supplementary Files

This is a list of supplementary files associated with this preprint. Click to download.

- [IPipeNatureMethodsSupplementsfinal.pdf](#)